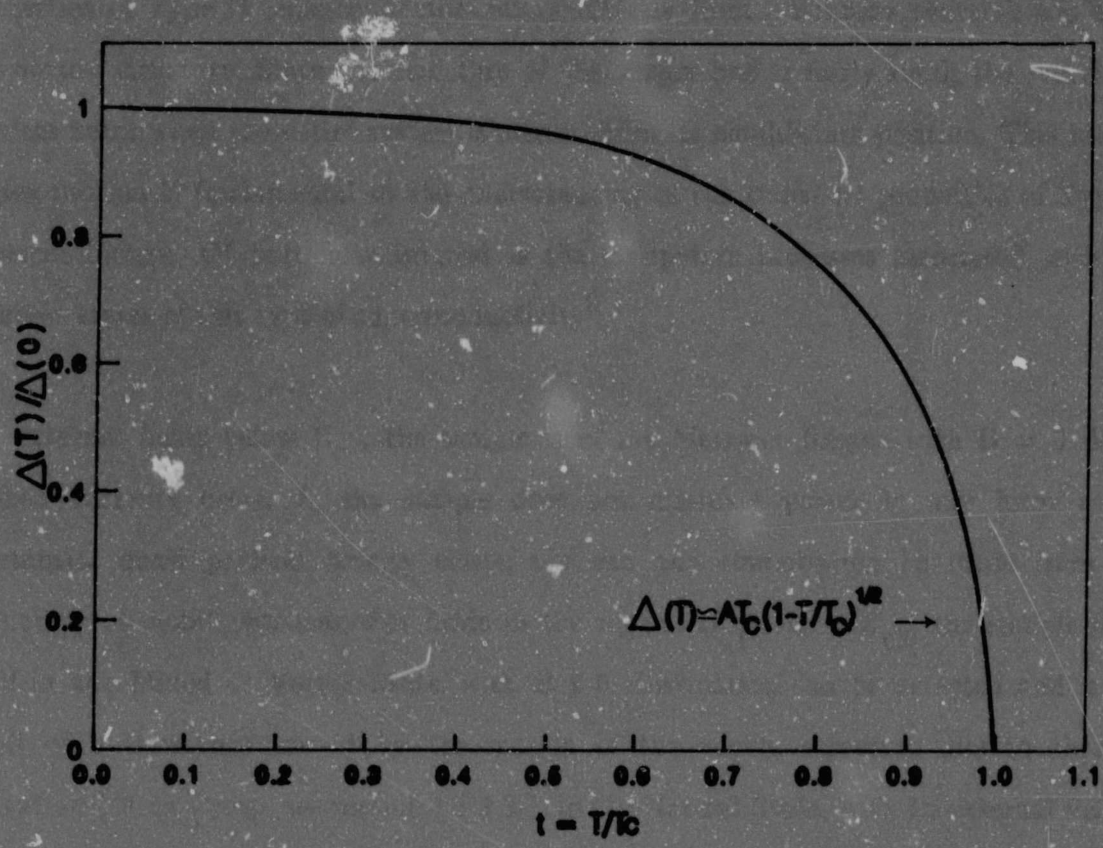

Figure 1.1.3 The BCS reduced energy gap versus reduced temperature. Just below T_c, $\Delta(T)$ is approximated by $\Delta(T) \simeq AT_c(1-T/T_c)^{1/2}$.

1.1.3 Flux Dynamics and Pinning

1.1.3.1 Type II Magnetic Flux Structure and Dissipation

Properties of Type II Superconductors follow directly from Abrikosov characterization of the vortex structure. Since the structure of the vortex line is fairly rigid, the individual vortices react when the entire system is altered from its equilibrium position. This idea of vortex motion is fundamental to the understanding of the transport properties of Type II Superconductors. Of particular interest is the dissipative processes associated with the different states of this type of superconductivity[9].

For external fields below H_{c1}, the sample is in the **Meissner Region** with $B = 0$. With applied currents below J_c the sample does not dissipate power in any form as no substantial quasi–particle density exists, nor can any contribution be made from the possibility of mobile vortices. For fields in the region, $H_{c1} < H < H_{c2}$, the sample finds itself in the **Mixed** or **Vortex State**, with $B \neq 0$. Dissipation can be detected and is the result of a resistance caused by the motion of the vortex structure due to thermal activation (Flux Creep, see section 1.1.3.3). In the **Normal State**, with an external field $H > H_{c2}$, quasi–particle scattering processes dominate the dissipation observed as all condensate should no longer exist.

1.1.3.2 Pinning

In Type II superconductivity, various lattice defects are inherent in the samples (essentially in the dirty limit), due to the formation of compounds. These sample inhomogeneities and defects pin down the flux lines and enable the sample to form

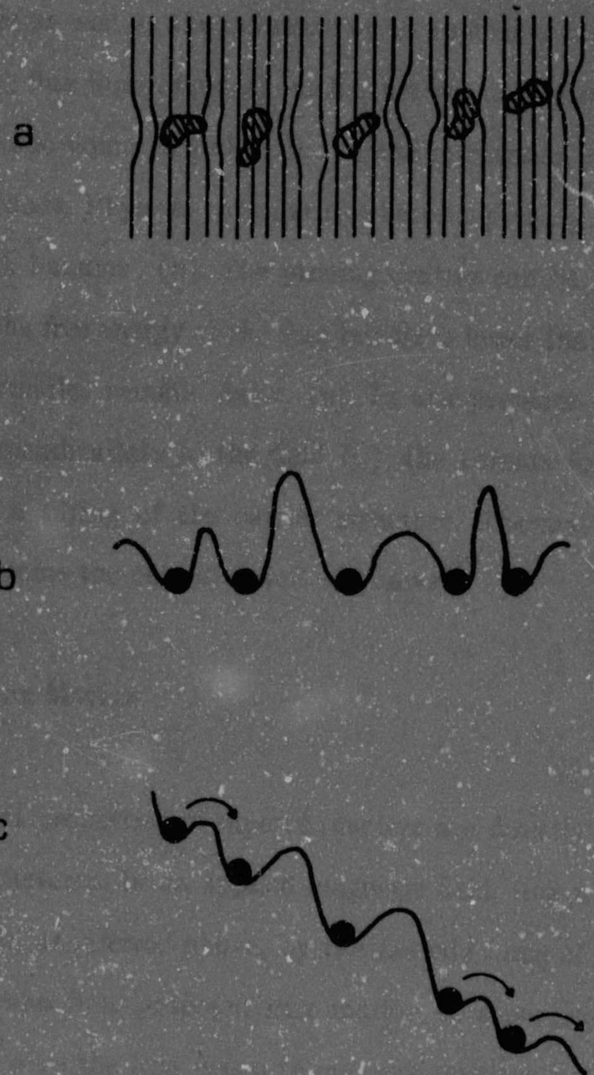

Figure 1.1.4 Kim's model of flux pinning in Type II superconductivity: a) Flux bundles pinned by material defects and inhomogeneities; b) Pinning centres act as the minima of local potential wells; c) With the addition of a Lorentz Force the potential well construction is tilted so that flux creep can occur aided by thermal activation.

non–uniform densities of flux lines more readily. Figure 1.1.4 represents schematically the pinning of flux bundles as well as the influence of an applied Lorentz force on the pinning barriers. (a): When the flux lines approach each other within a distance of λ (penetration depth), they can become bound together due to the interaction between their fields and overlapping wave functions. Physical irregularities become pinning centres, (accumulating points), for these 'flux bundles'. (b): The pinning centres can be regarded as minima for potential wells where the free energy of the flux bundle is lower than the wall energy of the well and hence, the bundles remain static. (c): In the presence of a transport current density **J** (applied perpendicularly to the field **B**), the Lorentz force, $\mathbf{J} \times \mathbf{B}$, on the flux bundles will result in a tilting of the barrier structure. Thermal activation, $\mathbf{k_B}T$, now enables the flux to overcome the potential well and move.[12]

1.1.3.3 Flux Motion

The interesting transport properties of superconductors are directly related to the motion of the magnetic flux structures. In an applied magnetic field, flux motion may be induced by a thermal gradient or, as inferred above, by the Lorentz force of an electric current. It was Gorter[13] in 1957 who first proposed flux motion in superconductors as a resistive mechanism. Kim et al[14] were the first group to measure resistive behaviour of flux flow in the Type II superconductors. They concluded that the voltage observed by increasing the Lorentz force beyond the depinning threshold was linear in current and that the slope of $\partial V/\partial I$ could be interpreted as the flow rate of fluxons in the sample.

According to Huebener[15] a phenomenological equation for the motion of flux in a sample as described in figure 1.1.5 is :

$$(J_x \times B_z) - fn_s e(v_\varphi \times B_z) - \eta v_\varphi - f_p = 0 \qquad 1.1.16.$$

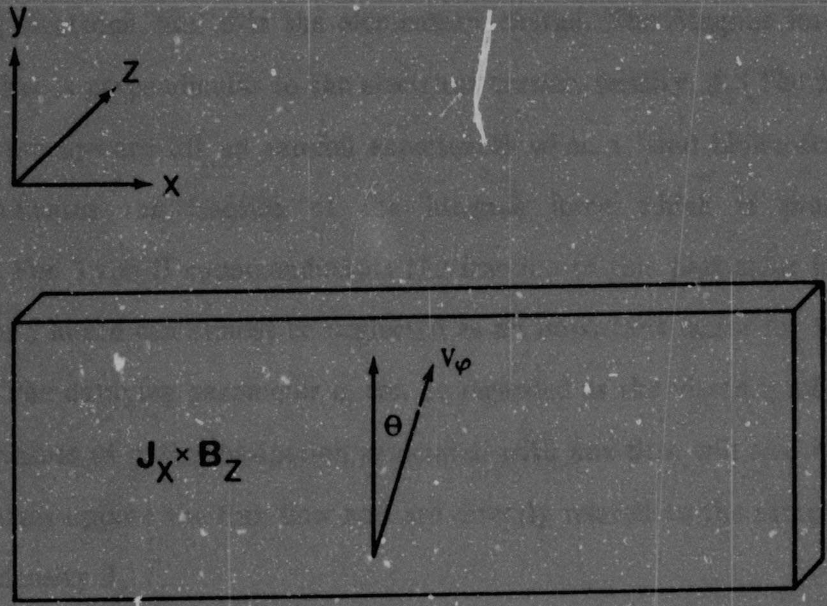

Figure 1.1.5 Huebener's model for describing the forces that govern vortex motion in a superconductor

If an electric current density of J_x is applied in the x direction and is sufficient to overcome the pinning f_p, the flux structure will move with a velocity v_φ in the direction given by the Hall angle θ between the y axis and v_φ. In the above equation it can be seen that the Lorentz force $(J_x \times B_z)$ is compensated by the Magnus force $fn_s e(v_\varphi \times B_z)$, the damping force ηv_φ, and the pinning force f_p. In the flux flow equation, n_s is the density of superconducting electrons, and e is the elementary charge. The Magnus force results in vortex motion that is perpendicular to the electrical current density, J, (The Magnus force is analogous to the upward lift an aerofoil experiences when a wind blows across it). The prefactor, f, indicates the fraction of the Magnus force which is present in the superconductor. For Type II superconductors the fraction of this particular force is much smaller than 1 and hence can almost be neglected as an important factor for the motion of flux structures. The damping parameter η, can be regarded as the viscosity of the material and for smaller values of η, the dissipation associated with flux flow will also be reduced[14]. The pinning centres oppose the flux flow and are directly related to the sample dependent critical current density J_c.

The resistance or dissipation associated with the flux flow is dependent on the viscous drag of the vortex motion. The derivation below follows the method outlined by Tinkham[16]. The damping force per unit length of a vortex line moving with velocity v_φ is $-\eta v_\varphi$. Equating this to the Lorentz driving force gives,

$$J \cdot \phi_0 = \eta \cdot v_\varphi \qquad 1.1.17.$$

The flux flow resistivity defined as $\rho_f = E/J = B\phi_0/\eta$, makes it necessary to express η in energetic terms by noting that the rate of energy dissipation per unit length of vortex is

$$W = -F \cdot v_\varphi = \eta v_\varphi^{\,2} \qquad 1.1.18.$$

The approach, henceforth, to find the dissipation due to a moving vortex is based on Bardeen and Stephen's model[17]. The uniform electric field inside a vortex core (of radius a) is

$$E_{core} = v_{\varphi}\phi_o/2\pi a^2 \qquad 1.1.19.$$

Given the electric field of the individual core, the dissipation of energy per unit length of core is

$$W_{core} = \pi a^2 \sigma_N E^2_{core} = v^2_{\varphi}\phi^2_o/4\pi a^2 \rho_N \qquad 1.1.20.$$

where σ_N is the normal–state conductivity (ρ_N the corresponding resistivity). Near T_c there will be as much dissipation outside the core as inside, and to maintain the simplicity of the model a factor of 2 is added to W_{core}. W_{core} is equated to the result 1.1.18 to obtain,

$$\eta = \phi^2_o/2\pi a^2 \rho_N \qquad 1.1.21.$$

Substituting into the above expression for ρ_f, using the fact that $H_{c2} = \phi_o/2\pi\xi^2$, and $a \simeq \xi$, $B \simeq H$ in the mixed state:

$$\rho_f/\rho_N = 2\pi a^2 B/\phi_o = H/H_{c2} \qquad 1.1.22.$$

An important characteristic of transport in superconductors is the dissipation associated with steady state flux motion. The moving flux induces an electric field according to Faraday's law of induction:

$$E = -\nabla V = -(v_{\varphi} \times B) \qquad 1.1.23.$$

where V is the measured voltage, and for the specific geometry of figure 1.1.5, the $\nu_{\varphi y}$ component causes this voltage and the $\nu_{\varphi x}$ component causes the Hall voltage. The motion of flux through a sample is associated with the transport of entropy. Vortices moving through a sample in a steady direction are created at the first boundary encountered and are annihilated at the next boundary. This process of creation and annihilation results in the absorption of heat at the creation point and emission of heat at the annihilation point, hence, thermal gradients are established between the sample edges. This particular effect can be minimized greatly by the use of a disc–shaped sample[15] where the current density J, flows radially (see figure 1.1.6 below). The rim and centre of the disc ideally have higher critical currents and tend towards the normal state sooner than the interior of the sample.This phenomenon is important if the disc is to have the property of radial equipotentiality.

The dissipation through flux flow in a superconductor is adverse to most technological applications and therefore samples with very high concentration of pinning centres are needed to increase the critical current density J_c. The model of Anderson[10] essentially deals with the behaviour of these hard superconductors in the early stages of flux motion. What Anderson proposed as the hop rate of flux bundles is the concept of flux creep and the predicted creep frequency is:

$$\nu_{\varphi} = \nu_o \exp(-U_o/k_B T) \qquad 1.1.24$$

where U_o is the activation energy necessary to overcome the pinning force and ν_o a prefactor. This is not a critical state model where the motion of flux cannot be described in terms of a steady state flow.

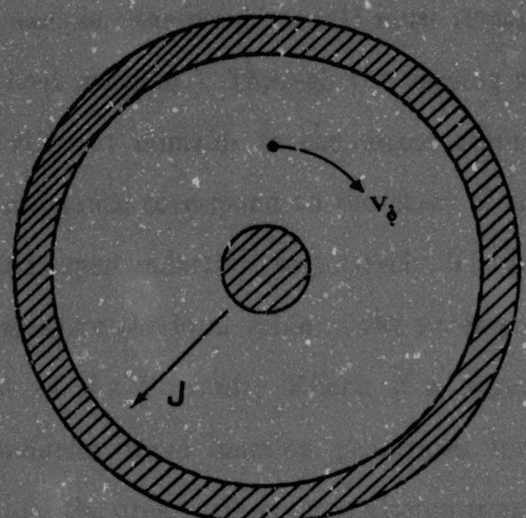

Figure 1.1.6 The disc geometry, where the current flows radially from the centre to the rim, and during flux flow, the vortices perform a continuous circular motion around the centre. The crosshatched sections consist of areas with a critical current much larger than that of the material between these sections; necessary to ensure equipotentiality in a radial direction.

1.1.4 Experimental Techniques and Observations

1.1.4.1 Sharvin Point Contact

A particularly useful technique for studying the dynamics of flux structures and the energy gap , is the Sharvin Point geometry[20,21]. A metal point contact, of approximately 25 μm is welded to a superconducting sample, (the point contact must remain normal through the superconducting state of the host material). Through the varying resistance measured at the contact, the motion of different domains in the mixed state can be studied. The maxima and minima of the resistance correspond to the state of the material under the point contact being normal and superconducting, respectively. The point contact geometry was later shown to actually measure the local value of the order parameter at the point. The latter occurring because of the Proximity Effect: if a normal metal adjoins the superconductor, the superconductor wave function penetrates some distance into the normal metal (range $\simeq \xi_N$) and the order parameter is altered from its Ψ_∞ value, to zero. The above, is also related to Josephson's[22] predicted quantum tunneling of coherent superconducting pairs, between two superconductors, even in the absence of an excitation voltage. This was later extended to the boundary regions of Superconductor – Insulator – Superconductor in granular superconductors by Anderson and Rowell[23]. Exploiting the Sharvin point contact geometry further, Andreev reflection[24,25] is an experimental technique that provides evidence for pairing in the superconducting condensate, (see Figure 1.1.7). In the process of Andreev scattering, an electron incident on the metal–superconducting boundary combines with another electron in the normal metal and is absorbed into the condensate, leaving behind a hole in the normal metal. Provided that the condensate consists of pairs of electrons with opposite momentum and spin, the result of this process is the creation of a hole with momentum and spin exactly opposite to that of the incident electron. The observation at the point contact is an increased current due to

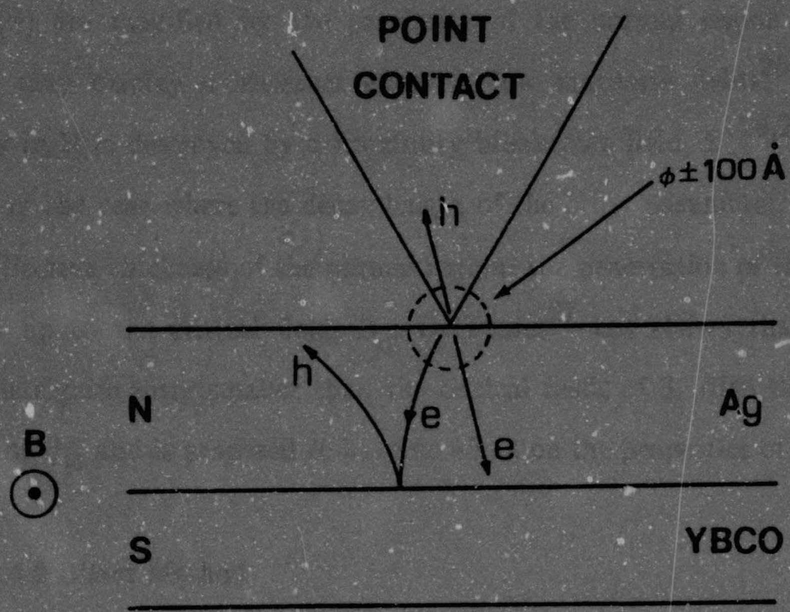

Figure 1.1.7 A Sharvin Point contact arrangement illustrates Andreev reflection. The applied magnetic field is orientated parallel to the normal–superconductor junction. A typical point contact size is of the order $\simeq 100$ Å.

accelerating electrons and a decrease in the contact resistance. The observation of Andreev reflection in accord with theoretical predictions would imply that the condensate is formed from pairs of electrons with zero net momentum.

The magnetic field dependence of superconducting properties in the region of a normal – superconducting boundary provide interesting effects. The critical fields of the superconductor (S) are modified by the proximity of the normal region (N), in some circumstances N may display a Meissner effect in low magnetic fields.[26] The induced superconductivity in N is destroyed by a Proximity breakdown field, B_o.[26,27] For Type II superconductors, in the case where the decay length of the order parameter, K^{-1} is of the order $\approx d_n$, the effective thickness of the normal region; the penetration of the field into N remains constant up to the critical field, B_o. DeGennes[27] has shown that this critical breakdown field is significantly smaller than the critical fields of S. Also the value of B_o depends strongly on d_N and is proposed to have no effect on the properties of S.

1.1.4.2 Bitter Method

An attractive method for observing the flux line patterns induced under the influence of vortex motion is the Bitter method. The existence of magnetic domains in ferromagnetic materials was shown by Bitter in 1931 using this method. This technique involves the use of small colloidal particles of a ferromagnetic material, which are attracted to the domain wall by the inhomogeneities in the magnetic field at the walls on the surface of the sample. The pattern of the particles are then examined with the aid of a microscope. Haenssler and Rinderer[28] extended this method to investigate the intermediate state in Type I superconductivity. Using the superconducting powder technique, the drift effect of propagating flux bundles, correlated with the Hall effect, they showed that spiral patterns resulted and terminated in the centre of the disc geometry. The Bitter method was used for a convincing demonstration of current induced flux flow in Type II superconductors by Träuble and Essmann.[29]

1.2 Physical Properties of High Temperature Superconductors

In 1986, Muller and Bednortz[30] revealed that at temperatures higher than 30 K the ceramic compound of Lanthanum and copper oxide (La_2CuO_4) goes into a superconducting state. Early in 1987, Wu et al[31], managed to form a sintered compound of Yttrium Copper oxide that had a transitional temperature of close to 90 K. Very soon compounds were produced by other groups verifying the new found High–T_c Superconductors, (High – T_c's). With the advent of these new copper oxide superconductors displaying very little dissipation below the boiling point of liquid nitrogen (77 K), the technological benefits became apparent. However, vast scientific resources were poured into the investigation of High T_c superconductors as the validity of conventional theories were questioned.

In the BCS theory of conventional Type II superconductors electrons are bound in Cooper pairs by an electron–phonon interaction (i.e. phonon mediated pairing). With the BCS theory and available phonon energies for these systems, it was difficult to account for the very high T_c values, using a strict phonon mediated pairing mechanism. The pairing mechanism is not yet clear for these materials and some experiments have indicated that the mechanism may not be phonon mediated at all. In addition to the above, the large spatial anisotropy due to the copper oxide plane structures, raised questions concerning the confinement of the charge transport. In the sections below (1.2.1) the author has only included the properties and theories of high T_c superconductivity that is pertinent to this study (with special reference to the $YBa_2Cu_3O_{7-\delta}$ structure).

1.2.1 Distinguishing Properties of High T_c Superconductors

The copper oxide superconductors are characterised by large unit cell volumes and a pronounced layer anisotropy. The properties of high – T_c superconductors differ essentially from the properties of conventional superconductors described by the BCS theory. The most important differences are listed below:

i) Anisotropy due to the layered structure caused by tripling the unit cell along the c–axis is an important characteristic of High T_c's. Large anisotropy becomes evident in the appreciable difference of coherence length for the direction along the c axis and directions perpendicular to it. The 2 or 3 Cu–O planes that constitute a unit cell include a number of current carriers (quasi–particles), usually holes which appear under appropriate oxygen doping. It has been shown that the Cu–O planes play an important role in the superconductivity of High–T_c's. The separation between Cu–O planes is however larger than the corresponding coherence length. Thus the superconducting coherence in the c direction is weak. This anisotropy results in interesting fluctuation effects due to the reduced dimensionality of the system. Reduced dimensionality can be understood in terms of the Mean Field Theory, where in conventional superconductors there exist very high concentrations of carriers in the 'coherence' volume, as opposed to the very low numbers of carriers ($n < 10$) for the High–T_c materials.

ii) The coherence length of high–T_c superconductors is very small, ($\xi_{ab} \simeq 15$ Å), approximately 10^3 times smaller than in conventional systems ; and in characterising the spatial stretching of the wave function of a Cooper pair, points towards a strong coupling of electrons in the pair. It is this **strong–coupling** that leads to the high critical transition temperatures.

iii) BCS theory predicts a superconducting energy gap given by eq. 1.1.14 above, wherein no allowed states occur. There has been evidence suggesting that a non–zero energy gap, (Psuedo–gap), exists in high–T_c's. Photoelectron Spectroscopy (PES) results